Published in final edited form as:
Neurobiol Aging. 2012 May ; 33(5): 1001.e1–1001.e6. doi:10.1016/j.neurobiolaging.2011.03.011.

Altered Ryanodine Receptor Expression in Mild Cognitive Impairment and Alzheimer's Disease

Angela Bruno[1], **Jeff Huang**[1], **David A. Bennett**[3], **Robert Marr**[1], **Michelle L. Hastings**[2,*], and **Grace E. Stutzmann**[1]

[1] Department of Neuroscience, Rosalind Franklin University/The Chicago Medical School, 3333 Green Bay Road, North Chicago IL 60064

[2] Department of Cell Biology and Anatomy, Rosalind Franklin University/The Chicago Medical School, 3333 Green Bay Road, North Chicago IL 60064

[3] Rush Alzheimer's Disease Center, Chicago, Illinois, Department of Neurological Sciences, Rush University Medical Center, Chicago, Illinois

Abstract

Intracellular Ca^{2+} dysregulation is an underlying component of Alzheimer's disease (AD) pathophysiology, and recent evidence implicates the ryanodine receptor (RyR) in the disease pathway. Three genes code for different RyR isoforms and each gene transcript gives rise to several alternatively spliced mRNAs. These variants confer distinct functionality to the RyR channel, such as altering Ca^{2+} release properties or subcellular localization. Changes in RyR isoform expression and alternative splicing have not been examined for potential roles in AD pathogenesis. Here, we compare mRNA levels of the RyR2 and RyR3 isoforms as well as specific alternatively spliced variants across vulnerable brain regions from postmortem samples of individuals with no cognitive impairment (NCI), mild cognitive impairment (MCI) and AD. We find an increase in RyR2 transcripts in MCI brains compared to NCI. In addition, there is a reduction in a RyR2 splice variant, associated with an anti-apoptotic function, in MCI and AD brains. These alterations in RyR expression at early disease stages may reflect the onset of pathologic mechanisms leading to later neurodegeneration.

Keywords

alternative splicing; Alzheimer's disease; apoptosis; calcium; endoplasmic reticulum; mild cognitive impairment; pre-mRNA splicing; ryanodine receptor

1. Introduction

Alzheimer's disease (AD) is characterized histologically by amyloid and tau deposits, and cognitively by impaired memory function. Although the etiology of AD is unknown, the

*Corresponding author: Michelle L. Hastings, Ph.D, Department of Cell Biology and Anatomy, Rosalind Franklin University/The Chicago Medical School, 3333 Green Bay Road, North Chicago, IL 60064, Michelle.hastings@rosalindfranklin.edu.

Disclosure Statement: No conflict of interest to declare.

contribution of aberrant endoplasmic reticulum (ER) Ca^{2+} release to AD progression is recognized as a pathogenic factor (Bezprozvanny and Mattson, 2008; Stutzmann, 2007; LaFerla, 2002). In particular, the ryanodine receptor (RyR), an ER-resident Ca^{2+} channel, is implicated in AD-linked Ca^{2+} dyshomeostasis (Smith et al., 2005; Stutzmann et al., 2006; Goussakov et al., 2010; Bezprozvanny and Mattson, 2008).

RyR is coded for by three genes: RyR1, 2 and 3. RyR2 and RyR3 are expressed in the brain at moderate to high levels while RyR1 is expressed at lower levels in restricted regions (Hertle and Yeckel, 2007). Tightly regulated RyR-mediated Ca^{2+} release is necessary for neuronal viability as well as higher cognitive functions, such as learning and memory, as well as the underlying synaptic plasticity via RyR2 and RyR3 isoforms (Zhao et al., 2000; Galeotti et al., 2008;Baker et al., 2010; Fitzjohn and Collingridge, 2002). By contrast, sustained Ca^{2+} dysregulation likely contributes to neurodegeneration and cognitive impairment (Stutzmann, 2007; Khachaturian, 1994). Consistent with this, upregulated RyR levels are found in human AD brains (Kelliher et al., 1999), while in animal models of AD, RyR2 and RyR3 isoforms are upregulated at early and late stages, respectively (Chakroborty et al., 2009, Supnet et al., 2006, Supnet et al., 2010, Zhang et al., 2010).

Prior to AD diagnosis, patients often present with a less severe condition termed mild-cognitive impairment (MCI) suggesting this may be a risk factor or precursor to AD (Ganguli et al., 2001; Peterson et al., 2001, Boyle et al., 2006). Little is known about Ca^{2+} dysregulation and RyR expression patterns in MCI. In healthy brains, RyR RNA transcripts are alternatively spliced, giving rise to mRNA variants which code for RyR isoforms with altered function, localization, and/or ligand affinity (Leeb et al., 1998, George et al., 2007, Jiang et al., 2003). However, the pattern of alternative RyR splice variants in AD and MCI brains has not been investigated. To address this, we examined changes in RyR isoforms and alternatively spliced variants in samples from persons with no cognitive impairment (NCI), MCI, and AD to determine if there are alterations in RyR patterns within vulnerable brain regions specific to dementia stage. We document a significant increase in RyR2 mRNA expression in human mid-temporal cortices of MCI brains, and differential expression of a RyR2 splice variant in MCI and AD brains that may increase vulnerability to apoptosis. Additionally, we reveal novel findings of differential alternative splicing of RyR3 across several brain regions.

2. Methods

Human brain samples

Postmortem samples were obtained through the Rush Religious Orders Study conducted by the Rush Alzheimer's Disease Center, Chicago, IL, taken from thirteen persons with NCI (age:74–90 years; mean age, 85.8, M:F 3:10), eleven with MCI (age, 75–92 years; mean age, 86.7, M:F 3:8), and eleven with AD (age, 80–95 years; mean age, 86.4, M:F 4:7). The postmortem intervals (PMIs) ranged from 1 hour – 27 hrs. Average PMIs for the NCI, MCI, and AD groups were 8.1, 7.0, and 7.6 hrs, respectively. Clinical diagnoses of NCI, MCI and AD have been previously reported in detail (Bennett et al., 2002).

RNA extraction and reverse transcription

Tissue samples were stored at −80° C and all samples were kept on dry ice during RNA extraction. For RNA isolation, 100 mg of tissue was homogenized in TRIZOL-Reagent (Invitrogen, Carlsbad, CA, USA) according to the manufacturer's protocol. Following DNAse treatment of 2 μg of total RNA (DNA Free Kit; Ambion), cDNA synthesis with random primers was performed using the High Capacity Reverse Transcription kit (Applied Biosystems).

Quantitative real-time PCR

Target gene expression was analyzed by real-time PCR using the 7500 RT PCR System and SYBR Green detection (Applied Biosystems). Cycling parameters were as follows: 2 min at 50° C, 10 min at 95° C, and then 36 cycles at 95° C for 15 s, followed by 60° C for 60 s. A dissociation phase was added to the end of each cycle to determine product purity. Beta 2 microglobulin (β2M) was used as a reference control gene (Coulson et al., 2008). Primer sequences for RyR isoforms are as follows:

RyR2 5′ TGCTGGCTTGGGGCTGGAGA3′ and 5′ACCATGGGCAGCGTCCACAG 3′

RyR3 5′ GACATGCGAGTCGGCTGGGC 3′ and 5′ GATGCCAACGCTGGCCCCTG 3′.

Primer specificities and product purity was supported by the presence of a single peak present on the dissociation curve for each primer set. Specificities were further validated by the presence of a single amplicon for each primer set at the predicted sizes after agarose gel electrophoresis of products with ethidium bromide staining. Each sample was evaluated in triplicate, and inter-run calibrators were employed as an indicator of systematic variation. Amplification data were analyzed using the comparative cycle threshold method after normalization to β2M. Primer efficiencies were validated prior to analysis using ΔCt, cDNA dilution assays.

Semi-quantitative PCR

PCR cycling parameters for RyR cDNA were: 10 min at 95° C, 40 cycles of 95° C for 30 s, 60° C for 60 s, 72 C for 60s. Reactions were allowed to run to completion for 5 min at 72 C, followed by a 4° C hold. Products were separated on agarose gels and stained with ethidium bromide. Data were recorded using a Gelprint 2000i CCD imaging system and quantitated with Metamorph Imaging 7.0 software. Primers were designed to flank the alternative splice sites. Primer sequences and product sizes: RyR2 30 bp 5′ CCATCAGTATGACACAGGC 3′ and 5′ CATTATTGTTGCGTCCTTGC 3′, with product sizes of 191 (+30) and 161 (−30) bp. For alternative splicing of the RyR3 isoform the primers are: RyR3 87 bp 5′ GAAGGTTGAGAAGCCGGAAG 3′ and 5′ CAGGGTTGGTGCCATATACC 3′ with product sizes of 295 (+87) bp and 208 (−87) bp. RyR3 82 bp 5′ CATTGATGAATCTGGACAGCAC 3′ and 5′ CCAGTGTGTCAACCATCTGC 3′ with product sizes of 320 (+82) bp and 258 (−82) bp.

To confirm splice variant identity, amplification products from the semi-quantitative PCR were extracted from gels, purified and sequenced at the Genomics Core Facility, Northwestern University, Chicago, IL.

Statisitcs

All analyses were performed with Origin 6.0 software. Data are represented as mean ± SEM. One-way ANOVA and the Tukey post hoc test were used to determine statistical significance.

Predicted Targeting Sequences/Signaling Peptides

The amino acid sequences corresponding to the alternatively spliced base pairs were probed for predicted targeting sequences using iPSORT (www.ipsort.hpc.jp).

3. Results

Regional alterations in RyR isoform expression levels in NCI, MCI and AD brains

Alterations in RyR levels have been documented in AD brains, although differences in specific RyR isoforms or their localization have not been investigated. Here, we examined relative mRNA expression levels of RyR2 and RyR3 using real-time PCR from mid-frontal, mid-temporal and caudate regions. Based on values normalized to the NCI group, there was a significant 2-fold increase in RyR2 mRNA expression in the mid-temporal cortex of MCI patients (one-way ANOVA; $p< 0.05$, Figure 1A) and a 1.8-fold increase in the mid-frontal cortex (one-way ANOVA; $p< 0.08$, Figure 1B). For RyR3 expression, there was a 1.6- and 1.5-fold increase in mid-frontal and mid-temporal expression, respectively, in AD (Figure 1C and 1D). The range of expression levels of RyR3 is not correlated with gender, age, MMSE score, Braak, CERAD, or Reagan scores ($p>0.05$). No differences were observed in expression of either isoform in the caudate in MCI or AD ($p>0.05$; not shown).

Changes in RyR isoform splice variants in MCI and AD

To determine whether changes in RyR isoform expression were accompanied by changes in alternative splice variants, we performed semi-quantitative PCR to detect relative levels of three RyR2 and RyR3 alternative splice variants. In addition, amino acid sequences corresponding to the alternatively spliced base pairs were analyzed for possible functional domains based on iPSORT.

RyR2+30 bp variant—A 30 bp cassette exon (+30) insert has been previously identified as a RyR2 alternatively spliced mRNA in adult human hippocampus, and was described in HL1 cardiomyocytes as having anti-apoptotic properties (George, 2007). Here, we reveal changes in alternative splicing of this exon across brain regions and disease states (Figures 2A, 2B, 2E). In NCI brains, RyR2 +30 comprised a greater proportion of total RyR2 in the mid-frontal cortex (0.41 ± 0.02, $p<0.05$) relative to the mid-temporal cortex, caudate and cerebellum (0.25 ± 0.02, 0.28 ± 0.02, 0.31 ± 0.02, respectively)(Figure 2A). Notably, the analysis revealed significantly less inclusion of the 30 bp insert in the mid-frontal cortex of MCI, (0.28 ± 0.03, $p<0.001$) and AD (0.33 ± 0.02, $p<0.05$) brains, respectively, relative to NCI (Figure 2B). Interestingly, there was a significantly higher level of inclusion in mid-temporal cortices of MCI (0.35 ± 0.01) but not AD (0.20 ± 0.02) brains relative to NCI (0.25 ± 0.02) (Figure 2A). In addition, iPSORT analysis indicates that the 30 bp exon codes amino acids predicted to be a signal peptide, although the specific target is unknown.

RyR3 exon 92 and 89 variants—A RyR3 mRNA transcript lacking the 87 base-pair exon 92 (Δ87), codes for a protein that functions as a dominant negative in mouse duodenum myocytes (Dabertrand, 2006). Here, we demonstrate that this splice variant is present in human brain, and, is expressed differentially across several regions (Figure 2C). In NCI brains, RyR3 Δ87 mRNA comprised a greater proportion of total RyR3 in the mid-frontal (0.84 ± 0.02), mid-temporal (0.83 ± 0.02) and cerebellum (0.82 ± 0.01), while less of this variant was detected in the caudate relative to the other regions (0.50 ± 0.03, $p < 0.05$). There was significantly less of the Δ87 variant in the mid-frontal but not mid-temporal cortices in AD brains (0.57 ± 0.02, $0.74 \pm .01$, respectively) relative to NCI (0.74 ± 0.03, 0.78 ± 0.02, respectively) (Figure 2D). There were no differences in MCI in either mid-frontal or mid-temporal cortices (0.71 ± 0.04, 0.75 ± 0.02, respectively). iPSORT supports that this splice variant is consistent with the amino acid sequence for a predicted signal peptide, although the target is not known.

Skipping of the 82 bp exon 89 (Δ82) in RyR3 mRNA results in a frameshift that creates a premature stop codon and a presumed subsequent truncated protein (Leeb, 1998). Relatively

more of this deletion is expressed in the caudate (0.46 ± 0.01), with lower levels in the cerebellum (0.22 ± 0.02) relative to mid-frontal and mid-temporal cortices (0.33 ± 0.01, 0.38 ± 0.02, respectively) (Figure 2E). There were no significant differences in AD susceptible regions between NCI and the disease states. Mid-frontal cortex values are 0.37 ± 0.03, 0.43 ± 0.01, and 0.41 ± 0.02 for NCI, MCI, and AD, respectively. Mid-temporal cortex values are 0.46 ± 0.02, 0.38 ± 0.04, 0.41 ± 0.03 for NCI, MCI and AD, respectively (Figure 2F).

4. Discussion

Clinical data shows a high conversion rate from MCI to AD, which strongly suggests they are closely linked conditions (Boyle et al, 2006). In this study, we reveal differences in specific RyR isoform expression levels among NCI, MCI, and AD brains which may signify a highly dynamic role of the RyR throughout various disease states. RyR2 mRNA levels are elevated in mid-temporal cortices in MCI, while the RyR3 levels are trending towards the increases observed in late-stage animal models of AD. Thus we posit that RyR2 is suspect early in the disease process while RyR3 may be implicated in later stages. This is consistent with previous research in mouse AD models (Chakroborty et al., 2009, Supnet et al., 2006; Zhang et al., 2010) and extends previous findings of an increase in [^{3}H]RyR binding in post-mortem early-stage AD brains (Kelliher, 1999).

We also found differential alternative splicing of RyR2 and RyR3 across mid-frontal cortex, mid-temporal cortex, caudate, and cerebellum. Notably, there is less inclusion of the RyR2 30 bp cassette exon in the mid-frontal cortices in MCI and AD brains. In contrast, we detect more inclusion of the exon in mid-temporal cortices of MCI but not AD brains. This splice variant has been shown to exert anti-apoptotic properties in HL-1 cardiomyocytes by reducing basal nuclear and cytosolic Ca^{2+} fluxes (George et al, 2007). Therefore, a reduction of this splice variant in AD and MCI brains may render these brain regions vulnerable to excitotoxicity and degeneration, thereby initiating or accelerating the disease process. The higher expression level in the mid-temporal cortex of MCI brains may reflect the roughly rostro-caudal progression of the disease process, or may reflect the complexity of splicing in the brain (Delacourte et al., 1999, Johnson et al., 2009). The 30 bp exon codes for a 10 amino acid insertion that disrupts a putative protein kinase C phosphorylation site (George et al, 2007). Although the amino acid sequence coded for by this 30-bp insert does not represent a known organelle targeting sequence, it is predicted as a signal peptide, and thus may affect subcellular localization within neurons.

We further identified a RyR3 splice variant not previously detected in human brain tissue. The 87 bp deletion corresponding to exon 92 in humans has been previously characterized in HEK 293 cells where it inhibited ER Ca^{2+} release when co-expressed with full-length RyR3, and decreased [^{3}H] binding when co-expressed with full-length RyR2 (Jiang et al JBC, 2003). We show that this splice variant mRNA is robustly expressed across 3 of the 4 brain regions examined, and that there is significantly lower expression in the mid-frontal cortex of AD brains (Fig. 2B). A similar regional expression pattern is found for the RyR3 82 bp splice variant, yet with no changes in disease states (Fig. 2C). We found abundantly more of the splice variant in the caudate and less of the variant in the cerebellum relative to mid-frontal and mid-temporal cortices. The exclusion of exon 90 from RyR3 mRNA leads to a premature termination codon resulting in the production of a truncated protein, thereby eliminating the ER retention signal predicted to reside in the 4th transmembrane domain (Leeb and Brenig, 1998).

We present here molecular findings consistent with, and in support of, previous work regarding RyR alterations in AD. In addition, we present significant findings of early

changes in expression of RyR2 in MCI in AD vulnerable regions, thereby offering novel opportunities for therapeutic intervention.

Acknowledgments

We thank Francine Jodelka and Megan Miller for technical assistance. This study was supported by NIH R01 AG030205, and AHAF to G.E.S and NIH RO1 NS069759 to M.H.

References

Baker KD, Edwards TM, Rickard NS. A ryanodine receptor agonist promotes the consolidation of long-term memory in young chicks. Behav Brain Res. 2009; 206:143–146. [PubMed: 19716384]

Bennett DA, Wilson RS, Schneider JA, Evans DA, Beckett LA, Aggarwal NT, Barnes LL, Fox JH, Bach J. Natural history of mild cognitive impairment in older persons. Neurology. 2002; 59:198–205. [PubMed: 12136057]

Bennett DA, Schneider JA, Bienias JL, Evans DA, Wilson RS. Mild cognitive impairment is related to Alzheimer disease pathology and cerebral infarctions. Neurology. 2005; 64:834–841. [PubMed: 15753419]

Bezprozvanny I, Mattson MP. Neuronal calcium mishandling and the pathogenesis of Alzheimer's disease. TINS. 2008; 31:454–463. [PubMed: 18675468]

Boyle P, Wilson R, Aggarwal N, Tang Y, Bennett D. Mild cognitive impairment: risk of Alzheimer disease and rate of cognitive decline. Neurology. 2006; (3):441–445. [PubMed: 16894105]

Chakroborty S, Goussakov I, Miller MB, Stutzmann GE. Deviant ryanodine receptor-mediated calcium release resets synaptic homeostasis in presymptomatic 3xTg-AD mice. J Neurosci. 2009; 29:9458–9470. [PubMed: 19641109]

Coulson DT, Brockbank S, Quinn JG, Murphy S, Ravid R, Irvine GB, Johnston JA. Identification of valid reference genes for the normalization of RT qPCR gene expression data in human brain tissue. BMC Mol Biol. 2008; 9:46. [PubMed: 18460208]

Dabertrand F, Fritz N, Mironneau J, Macrez N, Morel JL. Role of RYR3 splice variants in calcium signaling in mouse nonpregnant and pregnant myometrium. Am J Physiol Cell Physiol. 2007; 293:848–854.

Delacourte A, David JP, Sergeant N, Buee L, Wattez A, Vermersch P, Ghozali F, Fallet-Bianco C, Pasquier F, Lebert F, Petit H, Di Menza C. The biochemical pathway of neurofibrillary degeneration in aging and Alzheimer's disease. Neurology. 1999; 52(6):1158–65. [PubMed: 10214737]

Fitzjohn SM, Collingridge GL. Calcium stores and synaptic plasticity. Cell Calcium. 2002; 32:405–411. [PubMed: 12543099]

Galeotti N, Quattrone A, Vivoli E, Norcini M, Bartolini A, Ghelardini C. Different involvement of type 1, 2, and 3 ryanodine receptors in memory processes. Learn Mem. 2008; 15:315–323. [PubMed: 18441289]

Ganguli M, Tangalos G, Cummings JL, DeKosky ST. Practice parameter: Early Detection of dementia: Mild cognitive impairment (an evidence-based review). Report of the Quality Standards Subcommittee of the American Academy of Neurology. Neurology. 2001; 56:1133–1142. [PubMed: 11342677]

George CH, Rogers SA, Bertrand BM, Tunwell RE, Thomas NL, Steele DS, Cox EV, Pepper C, Hazeel CJ, Claycomb WC, Lai FA. Alternative splicing of ryanodine receptors modulates cardiomyocyte Ca2+ signaling and susceptibility to apoptosis. Circ Res. 2007; 100:874–883. [PubMed: 17322175]

Goussakov I, Miller MB, Stutzmann GE. NMDA-mediated Ca2+ influx drives ryanodine receptor activation in dendrites of young Alzheimer's disease mice. Journal of Neuroscience. 2010; 30:12128–37. [PubMed: 20826675]

Hertle DN, Yeckel MF. Distribution of inositol-1,4,5-trisphosphate receptor isotypes and ryanodine receptor isotypes during maturation of the rat hippocampus. Neuroscience. 2007; 150:625–638. [PubMed: 17981403]

Jiang D, Xiao B, Li X, Chen SR. Smooth muscle tissues express a major dominant negative splice variant of the type 3 Ca2+ release channel (ryanodine receptor). J Biol Chem. 2003; 278:4763–4769. [PubMed: 12471029]

Johnson MB, Kawasawa YI, Mason CE, Krsnik Z, Coppola G, Bogdanović D, Geschwind DH, Mane SM, State MW, Sestan N. Functional and evolutionary insights into human brain development through global transcriptome analysis. Neuron. 2009; 62(4):494–509. [PubMed: 19477152]

Kelliher M, Fastbom J, Cowburn RF, Bonkale W, Ohm TG, Ravid R, Sorrentino V, O'Neill C. Alterations in the ryanodine receptor calcium release channel correlate with Alzheimer's disease neurofibrillary and beta-amyloid pathologies. Neuroscience. 1999; 92:499–513. [PubMed: 10408600]

Khachaturian ZS. Calcium hypothesis of Alzheimer's disease and brain aging. Ann N Y Acad Sci. 1994; 747:1–11. [PubMed: 7847664]

LaFerla F. Calcium dyshomeostasis and intracellular signalling in Alzheimer's disease. Nat Rev Neurosci. 2002; 3:862–872. [PubMed: 12415294]

Leeb T, Brenig B. cDNA cloning and sequencing of the human ryanodine receptor type 3 (RYR3) reveals a novel alternative splice site in the RYR3 gene. FEBS Letters. 1998; 423:367–370. [PubMed: 9515741]

Ma J, Hayek SM, Bhat MB. Membrane Topology and Membrane Retention of the Ryanodine Receptor Calcium Release Channel. Cell Biochemistry and Biophysics. 2004; 40:207–224. [PubMed: 15054223]

Petersen RC, Doody R, Kurz A, Mohs RC, Morris JC, Rabins PV, Ritchie K, Rossor M, Thal L, Winblad B. Current concepts in mild cognitive impairment. Archives of Neurology. 2001; 58(12): 1985–1992. [PubMed: 11735772]

Smith IF, Hitt B, Green KN, Oddo S, LaFerla FM. Enhanced caffeine-induced Ca2+ release in the 3xTg-AD mouse model of Alzheimer's disease. Journal of Neurochemistry. 2005; 94:1711–1718. [PubMed: 16156741]

Stutzmann GE, Smith I, Caccamo A, Oddo S, LaFerla FM, Parker I. Enhanced ryanodine receptor recruitment contributes to Ca2+ disruptions in young, adult and aged Alzheimer's disease mice. Journal of Neuroscience. 2006; 26:5180–5189. [PubMed: 16687509]

Stutzmann GE. The pathogenesis of Alzheimer disease: Is it a lifelong 'calciumopathy'? The Neuroscientist. 2007; 13:546–559. [PubMed: 17901262]

Supnet C, Noonan C, Richard K, Bradley J, Mayne M. Up-regulation of the type 3 ryanodine receptor is neuroprotective in the TgCRND8 mouse model of Alzheimer's disease. Journal of Neurochemistry. 2010; 112(2):356–365. [PubMed: 19903243]

Supnet C, Grant J, Kong H, Westaway D, Mayne M. Amyloid-beta-(1-42) increases ryanodine receptor-3 expression and function in neurons of TgCRND8 mice. J Biol Chem. 2006; 281:38440–38447. [PubMed: 17050533]

Zhang H, Sun S, Herreman A, De Strooper B, Bezprozvanny I. Role of Presenilins in Neuronal Calcium Homeostasis. J Neurosci. 2010; 30(25):8566–8580. [PubMed: 20573903]

Zhao W, Meiri N, Xu H, Cavallaro S, Quattrone A, Zhang L, Alkon DL. Spatial learning induced changes in expression of the ryanodine type II receptor in the rat hippocampus. FASEB J. 2000; 14:290–300. [PubMed: 10657985]

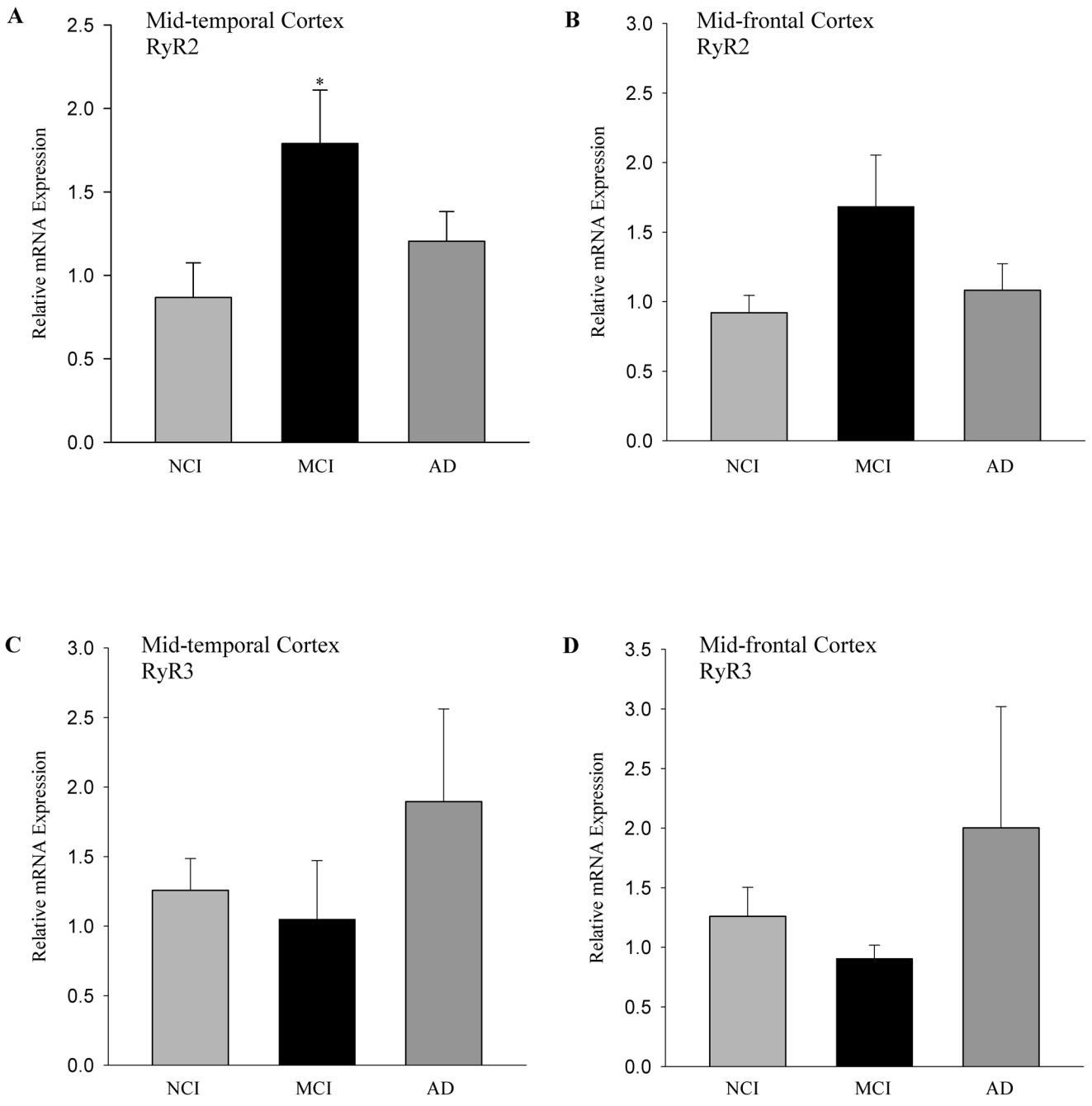

Figure 1.

RyR2 and RyR3 expression in the mid-temporal and mid-frontal cortices from NCI, MCI and AD brains. Bar graphs represent real-time PCR analysis of RyR2 mRNA in (**A**) mid-temporal and (**B**) mid-frontal cortex; and RyR3 mRNA from (**C**) mid-temporal and (**D**) mid-frontal cortex from NCI, MCI and AD brains. RyR mRNA levels were normalized to β2M. *$p < 0.05$, significantly different from NCI. Error bars represent ± SEM.

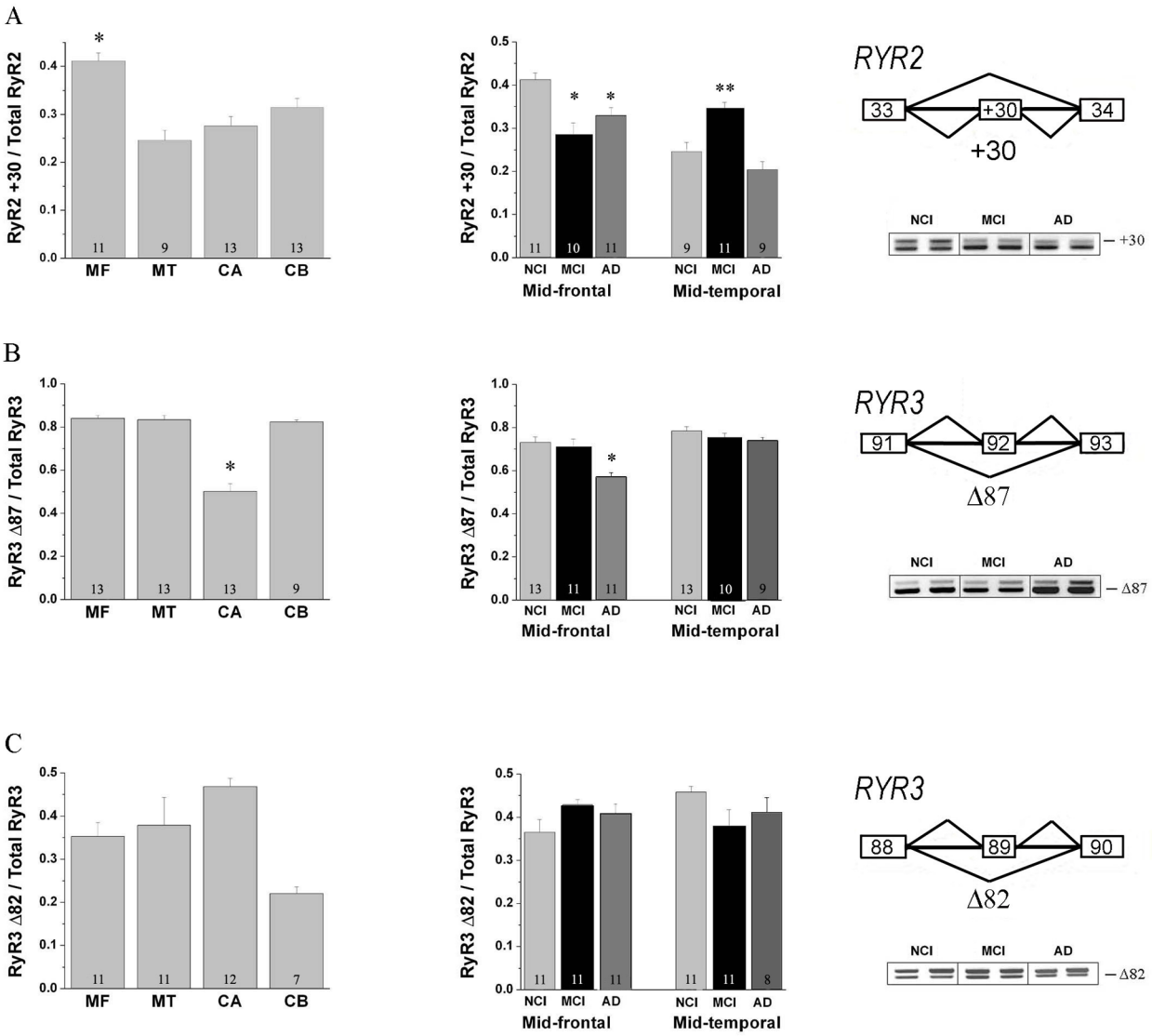

Figure 2.

Differential expression of splice variants across brain regions and disease states. Relative RT-PCR expression levels of the (**A**) RyR2 +30 splice variant (**B**) RyR3 Δ87bp splice variant and (**C**) RyR3 82bp splice variant across brain regions. Splice variants are graphed as the ratiometric density of RyR total. **Left panel**: Bar graphs represent relative mRNA transcript levels from the mid-frontal (MF), mid-temporal cortex (MT), caudate (CA) and cerebellum (CB) brain regions. **Middle panel**: mRNA transcript levels from mid-frontal cortex and mid-temporal cortex from NCI (gray), MCI (black), and AD (dark gray) brains. *$p < 0.05$, **$p < 0.001$, significantly different from NCI. One-way ANOVA and Tukey post hoc were used to determine significance. Error bars represent ± SEM. **Right panel**: Diagram of the alternatively spliced region with exons represented as boxes and introns as lines. Diagonal lines represent alternative splicing pathways. Gel represents a typical image of PCR products. Gel shows two lanes each of products from NCI, MCI, and AD samples.